Performance Analysis of MMSE-Based Amplify and Forward Spatial Multiplexing MIMO Relaying Systems

Changick Song, *Student Member, IEEE*, Kyoung-Jae Lee, *Member, IEEE*, and Inkyu Lee, *Senior Member, IEEE*

***Abstract*—In this paper, we propose a general framework to quantify the average error probability of the minimum mean squared error based precoding schemes in amplify-and-forward relay networks where all nodes are equipped with multiple antennas. Especially, we investigate spatial multiplexing schemes which transmit multiple data streams simultaneously. Due to difficulty in finding an exact expression of the average error rate, we exploit the high signal-to-noise-ratio (SNR) based approach which allows a simple and accurate characterization of the performance. Then, we derive new closed form expressions for bit error rate performance of both the optimal source-relay joint precoding schemes and the optimal relay only precoding schemes in terms of a coding gain as well as a diversity gain. Taking a different pathloss in each hop into consideration, we evaluate the performance in a generalized environment. Through our analysis, we discuss several interesting observations and provide a helpful guideline for designing MMSE-based relaying systems. Monte-Carlo simulations show that our analytical work accurately predicts numerical results.**

***Index Terms*—Relay systems, MIMO, precoding, MMSE solution.**

I. Introduction

MULTIPLE-INPUT multiple-output (MIMO) systems have been a promising means to increase the link performance for wireless systems. Especially spatial multiplexing MIMO schemes enable extremely high spectral efficiencies by transmitting independent data streams simultaneously through multiple transmit antennas [1] [2]. Recently, relaying techniques have also garnered a significant research interest since the communication range and coverage can be extended by supporting areas where there are strong shadowing effects [3] [4]. These benefits make MIMO relaying techniques an important component for next generation wireless networks.

In practical relay networks, one important relay protocol is amplify-and-forward (AF) due to its simplicity which amplifies the signal transmitted from the source and forward it to the destination [5]. In AF MIMO relaying systems, many spatial multiplexing schemes have been developed according to different approaches. One of most popular criteria is the minimum mean squared error (MMSE) [6]–[11], because other common system quality measures such as signal-to-noise ratio (SNR) and bit error rate (BER) can be readily related to the mean squared error.

Recently, the authors in [6] have investigated the MMSE optimal relay only precoding scheme where no channel state information (CSI) is allowed at the source node. Then, allowing the additional CSI at the source, the authors in [7]–[10] have tried to solve the source-relay joint optimization problem using iterative methods such as a gradient descent algorithm[1]. More recently, a new design approach for the MMSE-based relaying system has been reported in [11] where the closed-form solution for the source-relay joint precoding schemes was provided, which is optimal in the high SNR regime. Nevertheless, none of these works studied important performance measures such as an outage or an average error rate.

In simple beamforming cases where at least one node among the source, the relay and the destination is equipped with a single antenna, an exact error probability can be evaluated as in [12]–[19]. For example, in [13]–[15], single antenna relay channels have been studied in various fading environments. Extending these results to multiple antenna systems, the authors in [16]–[19] have computed the performance metric for AF relaying systems where multiple antennas are used for beamforming at the source or the destination. In contrast, the case where all nodes are equipped with multiple antennas driving multiple data streams has not been considered, because it is quite difficult to acquire an exact expression of the random channel distribution for each stream. Moreover, even if such a distribution was found, the solution might be intractable in most cases, since the expectation operation should be carried out numerically.

In this paper, by extending [16]–[19] to the case which supports multiple data streams with multiple antennas at all nodes, we provide a new analytical framework on the average BER performance of both the optimal source-relay joint precoding (SR) schemes [7]–[11] and optimal relay only precoding (R-) schemes [6] [11]. Regarding the power constraint at the

Paper approved by N. Jindal, the Editor for MIMO Techniques of the IEEE Communications Society. Manuscript received July 16, 2010; revised December 17, 2010.

This work was supported in part by the National Research Foundation of Korea (NRF) grant funded by the Korea government (MEST) (No.2010-0017909), and in part by the Seoul R&BD program (WR080951).

This paper was presented in part at the IEEE International Conference on Communications (ICC), Cape Town, South Africa, May 2010.

C. Song and I. Lee are with the School of Electrical Engineering, Korea University, Seoul, Korea (e-mail: {generalsci, inkyu}@korea.ac.kr).

K.-J. Lee was with the School of Electrical Engineering, Korea University. He is now with the Wireless Networking and Communications Group (WNCG), Department of Electrical and Computer Engineering, The University of Texas at Austin, Austin, TX, USA (e-mail: kyoungjae@korea.ac.kr).

Digital Object Identifier 10.1109/TCOMM.2011.101011.100421

[1]In this case, the global optimal solution is still unknown, because the problem is generally non-convex.

transmit sides, i.e., the source and the relay, our analysis considers the maximum eigenvalue constraint [11] as well as the conventional norm power constraint [6]–[11], since the maximum eigenvalue constraint is also useful to control the dynamic range of the power amplifier at each transmit antenna. Note that as the MMSE optimization problem is equivalent to the SNR maximization with a single stream transmission, existing beamforming schemes over the AF MIMO relay channel [13]–[20] can be characterized as special cases in our analytical work.

To overcome the difficulty in deriving the channel distribution and to obtain an insightful closed-form expression for the average BER, we focus on the high SNR performance as in [21] and [22]. In addition, we extend our discussion to generalized channel environment considering different pathloss in each hop to present a more practical observation on how the location of the relay node affects the performance. Our analytical results accurately predict the performance gain determined by various key performance parameters, e.g., a CSI requirement, a precoding strategy, antenna configurations and the number of data streams, and provide a helpful guideline for designing MMSE-based relaying systems. One interesting observation made from our analysis is that when the relay is placed closer to either the source or the destination, an additional source or destination antenna can introduce a non-trivial performance improvement according to the relay location. Simulation results confirm that the proposed analytical results provide an accurate estimation for the average BER of spatial multiplexing relaying schemes under various practical situations.

The rest of the paper is organized as follows: Section II provides the signal model for AF MIMO relaying systems. In Section III, closed form expressions are presented for the high-SNR performance of SR schemes. Then the performance of R- schemes is quantified in Section IV. Section V illustrates numerical results supporting our analytical works. Finally, our conclusions are drawn in Section VI.

Throughout this paper, normal letters represent scalar quantities, boldface lowercase letters indicate vectors and boldface uppercase letters designate matrices. $\mathbb{C}$ and $\mathbb{R}_+$ denote the set of complex numbers and the set of positive real numbers, respectively. The superscript $(\cdot)^\dagger$ stands for conjugate transpose, $\mathcal{E}(\cdot)$ denotes the expectation operator and $\mathbf{I}_N$ indicates an $N \times N$ identity matrix. $\mathrm{tr}\,(\mathbf{A})$ and $|\mathbf{A}|$ represent the trace and the determinant of a matrix $\mathbf{A}$, respectively. $\lambda_{\max}(\mathbf{A})$ indicates the maximum eigenvalue of a matrix $\mathbf{A}$. Also we write $f(x)$ as $o\,(g(x))$ if $f(x)/g(x) \to 0$ as $x \to 0$.

II. Signal Model for Transceiver Designs in AF MIMO Relaying Systems

As shown in Figure 1, we consider a MIMO relaying system where one relay node helps the communications between the source and the destination. The distance between the relay and the destination is assumed to be θ times longer than that between the source and the relay. We also assume that the source, relay and destination nodes use N_t, N_r and N_d number of antennas, respectively, and no direct path is considered due to a large shadowing effect between the source and the destination. As we take a spatial multiplexing into account which transmits N_s data streams simultaneously, we assume $N_s \leq \min\{N_t, N_r, N_d\}$. Our discussion is restricted to the uncorrelated narrowband channel model.

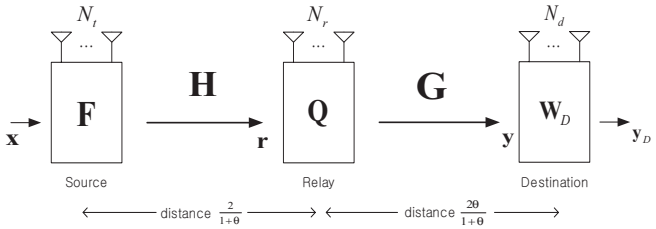

Fig. 1. System description for an AF MIMO relay network.

Data transmission occurs in two separate time slots. During the first time slot, the N_s dimensional transmit signal vector $\mathbf{x} \in \mathbb{C}^{N_s \times 1}$ with $\mathcal{E}(\mathbf{x}\mathbf{x}^\dagger) = \sigma_x^2 \mathbf{I}_{N_s}$ is precoded by the precoding matrix $\mathbf{F} \in \mathbb{C}^{N_t \times N_s}$, and transmitted to the relay node. Then the received signal $\mathbf{r} \in \mathbb{C}^{N_r \times 1}$ at the relay is given by $\mathbf{r} = \mathbf{H}\mathbf{x} + \mathbf{n}_1$, where $\mathbf{H} \in \mathbb{C}^{N_r \times N_t}$ denotes the first hop channel matrix of the source-to-relay link, and $\mathbf{n}_1$ indicates the complex normal Gaussian noise at the relay. In this case, denoting P_T as the total source transmit power, we can define the norm power constraint and the maximum eigenvalue constraint as $\mathcal{E}\big(\|\mathbf{F}\mathbf{x}\|^2\big) = \mathrm{tr}(\sigma_x^2 \mathbf{F}\mathbf{F}^H) \leq P_T$ and $\lambda_{\max}(\sigma_x^2 \mathbf{F}\mathbf{F}^H) \leq P_T/N_s$, respectively. Note that the eigenvalue constraint also satisfies the norm constraint while imposing a limit on the peak power of the transmit signals.

In the second time slot, the relay signal $\mathbf{r}$ is precoded by the relay transceiver $\mathbf{Q} \in \mathbb{C}^{N_r \times N_r}$ and transmitted to the destination. Then the received signal $\mathbf{y} \in \mathbb{C}^{N_d \times 1}$ is multiplied by the linear receiver $\mathbf{W}_D \in \mathbb{C}^{N_s \times N_d}$, and we have the final observation $\mathbf{y}_D \in \mathbb{C}^{N_s \times 1}$ as

$$\mathbf{y}_D = \mathbf{W}_D \mathbf{y} = \mathbf{W}_D(\mathbf{G}\mathbf{Q}\mathbf{H}\mathbf{F}\mathbf{x} + \mathbf{G}\mathbf{Q}\mathbf{n}_1 + \mathbf{n}_2),$$

where $\mathbf{G} \in \mathbb{C}^{N_d \times N_r}$ indicates the second hop channel matrix and $\mathbf{n}_2$ is the complex normal Gaussian noise at the destination. The optimal MMSE transceivers $\mathbf{F}$, $\mathbf{Q}$ and $\mathbf{W}_D$ have been investigated in [6]–[10] and more generally in [11]. In this paper, we follow the flow in [11] to simplify the presentation. From the MMSE point of view, the relay transceiver $\mathbf{Q}$ can be expanded as $\mathbf{Q} = \mathbf{B}\mathbf{L}_R$ where $\mathbf{L}_R$ and $\mathbf{B}$ represent the relay receiver and precoder, respectively. Then, in the high SNR regime, the relay constraints are also given by $\mathcal{E}(\|\mathbf{Q}\mathbf{r}\|^2) \simeq \mathrm{tr}(\sigma_x^2 \mathbf{B}\mathbf{B}^H) \leq P_R$ and $\lambda_{\max}(\sigma_x^2 \mathbf{B}\mathbf{B}^H) \leq P_R/N_s$ where P_R designates the total relay power.

The channel matrix in each hop can be further expressed as $\mathbf{H} = \sqrt{\eta_h}\tilde{\mathbf{H}}$ and $\mathbf{G} = \sqrt{\eta_g}\tilde{\mathbf{G}}$, where the entries of $\tilde{\mathbf{H}}$ and $\tilde{\mathbf{G}}$ are identically independent distributed (i.i.d.) complex normal Gaussian random variables. Each factor η_h and η_g contains the pathloss effect [23] [24] in each hop, and can be written as $\eta_h = \left(\frac{2}{1+\theta}\right)^{-\zeta_h}$ and $\eta_g = \left(\frac{2\theta}{1+\theta}\right)^{-\zeta_g}$ for $\theta \in \mathbb{R}_+$, where the scalars ζ_h and ζ_g denote the pathloss exponents. Here, we ignored the lognormal shadowing effect following the median pathloss model [23]. Note that the conventional equal distance channel model [6]–[11] is specified as a special case of $\theta = 1$.

Throughout the paper, we assume $\zeta_h = \zeta_g = \zeta$ and $P_T = P_R = P_0/2$ for simplicity, but the result can be easily extended

to more general cases. Here P_0 is defined as a total transmit power. Also, we define following eigenvalue decompositions as $\mathbf{H}^\dagger\mathbf{H} = \mathbf{V}_h\mathbf{\Lambda}_h\mathbf{V}_h^\dagger$ and $\mathbf{G}^\dagger\mathbf{G} = \mathbf{V}_g\mathbf{\Lambda}_g\mathbf{V}_g^\dagger$, where $\mathbf{\Lambda}_h$ and $\mathbf{\Lambda}_g$ represent diagonal matrices with eigenvalues $\lambda_{h,k}$ and $\lambda_{g,k}$ in a descending order on the main diagonal, respectively. We denote the matrix constructed by the first N_s columns of a unitary matrix $\mathbf{V}_h$ and $\mathbf{V}_g$ as $\overline{\mathbf{V}}_h$ and $\overline{\mathbf{V}}_g$, respectively. In the following, we describe the instantaneous SNR of the k-th substream for $k = 1, 2, \ldots, N_s$.

A. Instantaneous SNR of substreams

It has been shown in [11, Lemma 2] that from the MMSE point of view and for given $\mathbf{L}_R$ and $\mathbf{W}_D$, the error covariance matrix $\mathbf{E} \triangleq \mathcal{E}\big((\mathbf{y}_D - \mathbf{x})(\mathbf{y}_D - \mathbf{x})^\dagger\big)$ can be written at high SNR as

$$\mathbf{E} \;=\; \mathbf{E}_h + \mathbf{E}_g \tag{1}$$

where $\mathbf{E}_h \triangleq \big(\mathbf{F}^\dagger\mathbf{H}^\dagger\mathbf{H}\mathbf{F} + \sigma_x^{-2}\mathbf{I}_{N_s}\big)^{-1}$ and $\mathbf{E}_g \triangleq \big(\mathbf{B}^\dagger\mathbf{G}^\dagger\mathbf{G}\mathbf{B}+\sigma_x^{-2}\mathbf{I}_{N_s}\big)^{-1}$. Then, the joint MMSE optimization problem $(\hat{\mathbf{F}}, \hat{\mathbf{Q}}) = \min_{\mathbf{F},\mathbf{Q}} \mathrm{tr}(\mathbf{E})$ reduces to two individual problems $\hat{\mathbf{F}} = \arg\min_{\mathbf{F}} \mathrm{tr}(\mathbf{E}_h)$ and $\hat{\mathbf{B}} = \arg\min_{\mathbf{B}} \mathrm{tr}(\mathbf{E}_g)$.

Following this result, now we can easily express the instantaneous SNR of the k-th substream γ_k as [25] $\gamma_k = \sigma_x^2/E_k - 1 = \sigma_x^2/(E_{h,k} + E_{g,k}) - 1$, where E_k, $E_{h,k}$ and $E_{g,k}$ designate the (k,k)-th entry of the matrices $\mathbf{E}$, $\mathbf{E}_h$ and $\mathbf{E}_g$, respectively. Also defining $\gamma_{h,k} \triangleq \frac{\sigma_x^2}{E_{h,k}} - 1$ and $\gamma_{g,k} \triangleq \frac{\sigma_x^2}{E_{g,k}} - 1$, γ_k can be further approximated at high SNR as

$$\gamma_k = \frac{\gamma_{h,k}\gamma_{g,k} - 1}{\gamma_{h,k} + \gamma_{g,k} + 2} \approx \frac{\gamma_{h,k}\gamma_{g,k}}{\gamma_{h,k} + \gamma_{g,k}}. \tag{2}$$

Throughout the paper, the parameters defined in this section will serve as key factors for quantifying the average error performance.

III. Analytical Performance of Optimal Source-Relay Joint Precoding schemes

In this section, we develop a general framework to characterize the performance of SR schemes. For a wide family of Schur convex or concave cost functions, it is known that the optimal solution for the source-relay joint precoding designs which minimizes $\mathrm{tr}(\mathbf{E})$ follows the specific form as [11] [25]

$$\hat{\mathbf{F}} = \overline{\mathbf{V}}_h\mathbf{\Delta}_h^{1/2}\mathbf{N}_h \;\text{ and }\; \hat{\mathbf{B}} = \overline{\mathbf{V}}_g\mathbf{\Delta}_g^{1/2}\mathbf{N}_g, \tag{3}$$

where $\mathbf{N}_h \in \mathbb{C}^{N_s\times N_s}$ and $\mathbf{N}_g \in \mathbb{C}^{N_s\times N_s}$ are unitary rotation matrices, and $\mathbf{\Delta}_h \in \mathbb{C}^{N_s\times N_s}$ and $\mathbf{\Delta}_g \in \mathbb{C}^{N_s\times N_s}$ indicate diagonal matrices with entries being $\delta_{h,k}$ and $\delta_{g,k}$ for $k = 1, 2, \ldots, N_s$, respectively. Here $\delta_{h,k}$ and $\delta_{g,k}$ represent the power allocated to each substream at the source and the relay, respectively.

In the MMSE sense (or named sum-MSE minimization), power allocation strategy differs according to the power constraint at the transmit sides. In the following, we analyze the average error performance of SR schemes based on two celebrated constraints, the maximum eigenvalue constraint and the norm power constraint.

A. Source-Relay Joint Precoding with Maximum Eigenvalue Constraint

First, we consider the source and relay joint precoding scheme based on the maximum eigenvalue constraint (SR-MV). In this case, the power allocation factors are simply given by $\delta_{h,k} = 1$ and $\delta_{g,k} = 1$ for all k [11] [26], which is also regarded as a equal power allocation scheme. In addition, we have $\mathbf{N}_h = \mathbf{N}_g = \mathbf{I}_{N_s}$ by the Schur concavity of the cost function that minimizes the sum-MSE [25], which means that $\hat{\mathbf{F}} = \overline{\mathbf{V}}_h$ and $\hat{\mathbf{B}} = \overline{\mathbf{V}}_g$. Then we obtain the instantaneous SNR of the k-th substream in (2) as

$$\gamma_k = \sigma_x^2\frac{\lambda_{h,k}\lambda_{g,k}}{\lambda_{h,k} + \lambda_{g,k}} = \frac{P_0}{2N_s}\mu_k \tag{4}$$

where we define the harmonic mean of two channels' eigenvalues as $\mu_k \triangleq \lambda_{h,k}\lambda_{g,k}/(\lambda_{h,k} + \lambda_{g,k})$.

Once the instantaneous SNR is attained, we can calculate the average BER of the k-th substream solving the integral [27]

$$\overline{BER}_{\mathrm{mv},k} = \frac{\alpha}{\log_2 M}\int_0^\infty Q\left(\sqrt{\beta\gamma_k}\right) f_{\mu_k}(\mu_k)d\mu_k, \tag{5}$$

where M designates a modulation level, and α and β are modulation level dependent parameters given by $\alpha = 4(1 - 1/\sqrt{M})$ and $\beta = 3/(M-1)$. However, to solve the integral, we need to know the probability density function (PDF) $f_{\mu_k}(\mu_k)$ of the channel dependent random parameter μ_k. In fact, getting the exact PDF of the harmonic mean of arbitrary two random variables is very difficult, and even if such a PDF is available[2], the solution might be intractable in many cases, because it is too complicated as in [13] and [14]. In this paper, putting an emphasis on the high SNR region, we derive a simple and useful expression of the harmonic mean PDF.

In the high SNR regime, it is well known fact [21] that the average error performance mostly depends on the behavior of the PDF $f_{\mu_k}(\mu_k)$ of μ_k near zero ($\mu_k \to 0^+$), since otherwise the Q-function in (5) converges to zero. Also, it is known that the first-order expansion of the marginal PDFs of the k-th largest eigenvalues $\lambda_{h,k}$ and $\lambda_{g,k}$ of $\mathbf{H}^\dagger\mathbf{H}$ and $\mathbf{G}^\dagger\mathbf{G}$ are given by

$$\begin{aligned} f_{\lambda_{h,k}}(\lambda_{h,k}) \;&=\; a'_{h,k}\lambda_{h,k}^{d_{h,k}} + o\big(\lambda_{h,k}^{d_{h,k}}\big) \\ \text{and}\;\; f_{\lambda_{g,k}}(\lambda_{g,k}) \;&=\; a'_{g,k}\lambda_{g,k}^{d_{g,k}} + o\big(\lambda_{g,k}^{d_{g,k}}\big), \end{aligned} \tag{6}$$

where $d_{h,k} = (N_t - k + 1)(N_r - k + 1) - 1$, $d_{g,k} = (N_r - k + 1)(N_d - k + 1) - 1$, $a'_{h,k} = a_{h,k}\eta_h^{-(d_{h,k}+1)}$ and $a'_{g,k} = a_{g,k}\eta_g^{-(d_{g,k}+1)}$. Here the parameters $a_{h,k}$ and $a_{g,k}$ are found in [22] and [28]. Based on these facts, now in the following lemma, we derive a PDF of the harmonic mean of arbitrary two independent ordered eigenvalues.

Lemma 1: For small argument μ_k, i.e., $\mu_k \to 0^+$, the PDF of μ_k is given by

$$\begin{aligned} f_{\mu_k}(\mu_k) \;&=\; f_{\lambda_{h,k}}(\mu_k) + f_{\lambda_{g,k}}(\mu_k) \\ &=\; a'_{h,k}\mu_k^{d_{h,k}} + a'_{g,k}\mu_k^{d_{g,k}} + o\left(\mu_k^{\min(d_{h,k},d_{g,k})}\right). \end{aligned}$$

[2]In fact, the exact PDF of the harmonic mean has been derived in [13] and [14] for two i.i.d. exponential random variables and for two i.i.d. gamma random variables, respectively, but for two arbitrary ordered eigenvalues, it is still unknown.

Proof: See Appendix A. ∎

Now, using the result in Lemma 1, we can easily solve the integral in (5) for the average BER of k-th substream. Then, taking all substreams into account, the total average BER of SR-MV can be parameterized in terms of a diversity gain and a coding gain as follows.

Theorem 1: The total average BER performance of SR-MV is obtained by

$$\overline{BER}_{\text{mv}} = \begin{cases} (\mathcal{C}_h \cdot P_0)^{-\mathcal{D}_h} + o(P_0^{-\mathcal{D}_h}) & \text{if } N_t < N_d; \\ (\mathcal{C}_g \cdot P_0)^{-\mathcal{D}_g} + o(P_0^{-\mathcal{D}_g}) & \text{if } N_t > N_d; \\ (\mathcal{C} \cdot P_0)^{-\mathcal{D}} + o(P_0^{-\mathcal{D}}) & \text{if } N_t = N_d, \end{cases}$$

where the diversity gains are determined as $\mathcal{D}_h = d_{h,N_s} + 1$ and $\mathcal{D}_g = d_{g,N_s} + 1$. $\mathcal{D}$ represents the diversity gain for the case of $N_t = N_d$ such that $\mathcal{D} = \mathcal{D}_h = \mathcal{D}_g$. The coding gains $\mathcal{C}_h$, $\mathcal{C}_g$ and $\mathcal{C}$ are denoted by $\mathcal{C}_h = \frac{1}{2}\eta_h N_s^{1/\mathcal{D}_h - 1} G_c(0, a_{h,N_s}, d_{h,N_s})$, $\mathcal{C}_g = \frac{1}{2}\eta_g N_s^{1/\mathcal{D}_g - 1} G_c(0, a_{g,N_s}, d_{g,N_s})$ and $\mathcal{C} = (\mathcal{C}_h^{-\mathcal{D}} + \mathcal{C}_g^{-\mathcal{D}})^{-1/\mathcal{D}}$, respectively, where the function $G_c(\cdot,\cdot,\cdot)$ is defined as

$$G_c(\phi, a, d) \triangleq \beta \left(\frac{\alpha}{\log_2 M} \frac{a I(d, \beta\phi)}{\sqrt{2\pi}(d+1)} \right)^{-1/(d+1)}, \qquad (7)$$

and $I(d, \beta\phi) \triangleq \int_{\sqrt{\beta\phi}}^{\infty} e^{-x^2/2}(x^2 - \beta\phi)^{d+1} dx$.

Proof: See Appendix B. ∎

B. Source-Relay Joint Precoding with Norm Power Constraint based on MSE

In the high SNR regime, the power allocated to the k-th substream in the optimal source and relay joint precoding design with norm power constraint (SR-NC) [8] [11] can be written as

$$\begin{aligned} \delta_{h,k} &= \left(\tau(\sigma_x^2 \lambda_{h,k})^{-1/2} - (\sigma_x^2 \lambda_{h,k})^{-1}\right)^+ \\ \text{and } \delta_{g,k} &= \left(\kappa(\sigma_x^2 \lambda_{g,k})^{-1/2} - (\sigma_x^2 \lambda_{g,k})^{-1}\right)^+, \end{aligned} \qquad (8)$$

where τ and κ are chosen to meet the NC (i.e., $\sum_{k=1}^{N_s} \delta_{h,k} = N_s$ and $\sum_{k=1}^{N_s} \delta_{g,k} = N_s$), and $x^+ \triangleq \max(0, x)$. In addition, in the same manner as in the previous subsection, we have $\mathbf{N}_h = \mathbf{N}_g = \mathbf{I}_{N_s}$ by the Schur concavity of the cost function. Now, we analyze the total average BER performance of SR-NC. By exploiting the solutions in (8), we can show that SR-NC makes a non-trivial coding gain improvement over SR-MV. However it does not exhibit any diversity advantage, since waterfilling fashioned power allocations cannot change the diversity gain in each substream [22]. Therefore, we know that the total average BER of SR-NC also mainly depends on the BER of the N_s-th substream that has the worst diversity order. In the following lemma, we first parameterize the average BER of the N_s-th substream.

Lemma 2: The average BER of the N_s-th substream in SR-NC is given in the high SNR regime as

$$\begin{aligned} \overline{BER}_{\text{nc},N_s} = &(N_s \mathcal{C}_h \cdot P_0)^{-\mathcal{D}_h} + (N_s \mathcal{C}_g \cdot P_0)^{-\mathcal{D}_g} \\ &+ o(P_0^{-\min(\mathcal{D}_h, \mathcal{D}_g)}). \end{aligned}$$

Proof: See Appendix C. ∎

Then, averaging over N_s data symbols, the total average BER of SR-NC is obtained as follows.

Theorem 2: The total average BER performance of SR-NC is given by

$$\overline{BER}_{\text{nc}} = \begin{cases} (\mathcal{C}_{h,\text{nc}} \cdot P_0)^{-\mathcal{D}_h} + o(P_0^{-\mathcal{D}_h}) & \text{if } N_t < N_d; \\ (\mathcal{C}_{g,\text{nc}} \cdot P_0)^{-\mathcal{D}_g} + o(P_0^{-\mathcal{D}_g}) & \text{if } N_t > N_d; \\ (\mathcal{C}_{\text{nc}} \cdot P_0)^{-\mathcal{D}} + o(P_0^{-\mathcal{D}}) & \text{if } N_t = N_d, \end{cases}$$

where $\mathcal{C}_{h,\text{nc}} = N_s \mathcal{C}_h$ and $\mathcal{C}_{g,\text{nc}} = N_s \mathcal{C}_g$, and $\mathcal{C}_{\text{nc}}$ represents the coding gain for the case of $N_t = N_d$ given by $\mathcal{C}_{\text{nc}} = (\mathcal{C}_{h,\text{nc}}^{-\mathcal{D}} + \mathcal{C}_{g,\text{nc}}^{-\mathcal{D}})^{-1/\mathcal{D}}$.

Proof: The proof simply follows from Lemma 2 and Theorem 1. Details are trivial and omitted. ∎

C. Source-Relay Joint Precoding with Norm Power Constraint based on BER

Now, we complete the performance analysis of the source and relay joint optimal precoding designs by focusing on the minimum-BER based criterion which minimizes the maximum MSE (SR-BNC) [8] [11]. In this case, the power allocation parameters $\delta_{h,k}$ and $\delta_{g,k}$ follow the same solution as in (8). Also, denoting $\mathbf{Z} \in \mathbb{C}^{N_s \times N_s}$ as the discrete Fourier transform matrix, we have $\mathbf{N}_h = \mathbf{N}_g = \mathbf{Z}$ by the Schur convexity of the cost function [25], which ensures that all diagonal elements of the $\mathbf{E}$ in (1) have the same value. Now in the next theorem, we will derive the average BER of SR-BNC.

Theorem 3: The total average BER performance of SR-BNC is obtained as

$$\overline{BER}_{\text{bnc}} = \begin{cases} (\mathcal{C}_{h,\text{bnc}} \cdot P_0)^{-\mathcal{D}_h} + o(P_0^{-\mathcal{D}_h}) & \text{if } N_t < N_d; \\ (\mathcal{C}_{g,\text{bnc}} \cdot P_0)^{-\mathcal{D}_g} + o(P_0^{-\mathcal{D}_g}) & \text{if } N_t > N_d; \\ (\mathcal{C}_{\text{bnc}} \cdot P_0)^{-\mathcal{D}} + o(P_0^{-\mathcal{D}}) & \text{if } N_t = N_d, \end{cases}$$

where the coding gains $\mathcal{C}_{h,\text{bnc}}$ and $\mathcal{C}_{g,\text{bnc}}$ can be approximated as $\mathcal{C}_{h,\text{bnc}} = \frac{N_s}{2}\eta_h G_c(\beta(N_s - 1), a_{h,N_s}, d_{h,N_s})$ and $\mathcal{C}_{g,\text{bnc}} = \frac{N_s}{2}\eta_g G_c(\beta(N_s - 1), a_{g,N_s}, d_{g,N_s})$, respectively, and $\mathcal{C}_{\text{bnc}}$ represents the coding gain for the case of $N_t = N_d$ computed as $\mathcal{C}_{\text{bnc}} = (\mathcal{C}_{h,\text{bnc}}^{-\mathcal{D}} + \mathcal{C}_{g,\text{bnc}}^{-\mathcal{D}})^{-1/\mathcal{D}}$.

Proof: See Appendix D. ∎

D. Discussion

Now, we see from the analysis that the diversity order of SR schemes is determined by $(N_r - N_s + 1)\big(\min(N_t, N_d) - N_s + 1\big)$ which shows the tradeoff between the diversity and the number of spatial streams in two hop relay networks. Our results include existing works for beamforming schemes as special cases. For example, for the system with multiple antennas at the source and the destination, and a single antenna at the relay ($N_r = N_s = 1$), the diversity order is given by $\min(N_t, N_d)$ [18]. Also we see that the optimal beamforming strategy [20] ($N_s = 1$) exploits a full diversity order of the flat fading MIMO relay channel as $N_r \cdot \min(N_t, N_d)$. Also, it is clear from the analysis that for relaying systems with $N_r > \max(N_t, N_d)$, a higher diversity order can be achieved over the MMSE-based $N_t \times N_d$ closed-loop MIMO system[3] [25] [26].

[3]The diversity order of this conventional MIMO system has been derived as $(N_t - N_s + 1)(N_d - N_s + 1)$ [22] [29]

From Theorem 1 to 3, it is shown that for $N_t = N_d$, the coding gains $\mathcal{C}$, $\mathcal{C}_{\text{nc}}$ and $\mathcal{C}_{\text{bnc}}$ can be represented as a quasi-concave function of θ with inequality constraint $\theta \geq 0$ [30]. Since the feasible set ($\theta \in \mathbb{R}_+$) contains only one optimal point, we can always find the global optimal point as a closed form. By setting the gradient of each coding gain to zero, we see that the middle point ($\theta = 1$) achieves the optimum for all SR schemes. However, this result also implies that if the relay is located far from the middle point, we would suffer from a considerable performance loss as will be shown later. Our analysis demonstrates that in this case, we can make a much larger coding gain improvement by using an additional antenna either at the source or the destination as explained in the following.

Recently, the authors in [17] have shown that for $N_t = N_r = N_d = 1$, additional source antennas produce a 3 dB coding gain advantage irrespective of the number of increased antennas. From our analysis, we can generalize this to the system with multiple data streams. For example, suppose that N_t is increased from the case of $N_t = N_d = N$ while N_s and N_r are fixed. As the increment of N_t cannot create any diversity advantage, the diversity order stays with $\mathcal{D} = (N_r - N_s + 1)(N - N_s + 1)$. Thus, from Theorem 1, we can compute the coding gain advantage caused by an additional source antenna as $10\log(\mathcal{C}_g/\mathcal{C}) = \frac{10}{\mathcal{D}}\log\left(1+\theta^{-\zeta\mathcal{D}}\right)$ dB. On the contrary, if N_d is increased, we will get a $\frac{10}{\mathcal{D}}\log\left(1+\theta^{\zeta\mathcal{D}}\right)$ dB gain.

For $\theta = 1$, simply a $3/\mathcal{D}$ dB gain is obtained, which is inversely proportional to the diversity order. The maximum gain is only 3 dB at $\mathcal{D} = 1$. This result implies that for $\theta = 1$, increasing either N_t or N_d may not be useful, especially in the system with a high diversity order ($\mathcal{D} > 1$). In contrast, if we consider the different pathloss between two hops, a considerable performance improvement can be expected by adding an additional antenna at the source or the destination. As a specific example, if we assume $\theta = 2$ (i.e., relay is closer to the source), $\mathcal{D} = 1$, and $\zeta = 4$, then a $\frac{10}{\mathcal{D}}\log(1+\theta^{\zeta\mathcal{D}}) = 12.3$ dB gain can be obtained over the case of $N_t = N_d$ by using an additional antenna at the destination. On the contrary, if $\theta = 1/2$ (i.e., relay is closer to the destination), exactly the same gain can be drawn by increasing the source antenna. Note that these results stated so far hold for all SR schemes. Our results are also applicable to practical relaying strategies such as the relay selection method with geometric information of θ in a multi-relay network.

Theorem 2 and 3 illustrate that the NC-based schemes (i.e., SR-NC and SR-BNC) do not make any diversity advantage compared to the SR-MV, but can provide a non-negligible coding gain improvement. Actually, SR-NC attains a $10\log N_s$ dB gain over SR-MV, regardless of the diversity order. As N_s grows, the achievable gain will be higher. The most important feature to notice here is that when $N_t > N_d$, the norm constraint based power allocation at the source as in (8) which requires higher complexity than the eigenvalue constraint may not be efficient, because the overall performance is dominated by the relay-destination link.

From the definition in (7), $G_c(\phi, a, d)$ is a monotonic increasing function of ϕ. Also SR-BNC has $\phi = N_s - 1$ while $\phi = 0$ in SR-NC. Hence, the BER-based optimized scheme introduces a further coding gain over MSE-based ones. For instance, for $\theta = 1$ and QPSK transmission with $N_t = N_r = N_d = N_s = 4$, the coding gains are computed as $\mathcal{C} = \frac{1}{4}G_c(0,4,0) = 0.125$, $\mathcal{C}_{\text{nc}} = G_c(0,4,0) = 0.5$ and $\mathcal{C}_{\text{bnc}} = G_c(3,4,0) = 3.52$. In other words, SR-NC and SR-BNC exhibit 6dB and 14.5dB gains over SR-MV, respectively. All these observations made in this section will be confirmed by simulation results in Section V.

IV. Analytical Performance of Optimal Relay only Precoding schemes

The SR schemes studied so far provide the optimal performance in the relay network, but full CSI is required at the source. Moreover, SR schemes may impose a large processing complexity on the system. For these practical reasons, relay only precoding schemes have widely been investigated [6] [11] and the analysis for them is important as well.

Now in the following, we analyze the high SNR performance of R- schemes with two different criteria: maximum eigenvalue constraint (R-MV) [11] and norm power constraint (R-NC) [6]. Due to no CSI at the source node and the Schur concavity of the cost function, the optimal solutions in (3) are given by $\hat{\mathbf{F}} = \mathbf{I}_{N_t}$ and $\hat{\mathbf{B}} = \overline{\mathbf{V}}_g \mathbf{\Delta}_g^{1/2}$. Therefore, in this section, we basically assume $N_t = N_s \leq \min(N_r, N_d)$.

First, let us consider the R-MV. With the eigenvalue constraint, the optimal relay precoder is expressed as $\hat{\mathbf{B}} = \overline{\mathbf{V}}_g$, since $\delta_{g,k} = 1$ for all k. Then the average performance of R-MV can be presented as in the following theorem.

Theorem 4: The total average BER of R-MV is given by

$$\overline{BER}^R_{\text{mv}} = \begin{cases} \left(\bar{\mathcal{C}}_h \cdot P_0\right)^{-\bar{\mathcal{D}}} + o(P_0^{-\bar{\mathcal{D}}}) & \text{if } N_t < N_d; \\ \left(\bar{\mathcal{C}} \cdot P_0\right)^{-\bar{\mathcal{D}}} + o(P_0^{-\bar{\mathcal{D}}}) & \text{if } N_t = N_d, \end{cases}$$

where we denote the diversity gain as $\bar{\mathcal{D}} = N_r - N_t + 1$, and the coding gains as $\bar{\mathcal{C}}_h = \frac{1}{2}\eta_h N_t^{-1} G_c(0, \bar{a}_h, \bar{d}_h)$ and $\bar{\mathcal{C}} = (\bar{\mathcal{C}}_h^{-\bar{\mathcal{D}}} + \mathcal{C}_g^{-\bar{\mathcal{D}}})^{-1/\bar{\mathcal{D}}}$. Here $\bar{d}_h$ and $\bar{a}_h$ denotes $\bar{d}_h = N_r - N_t$ and $\bar{a}_h = (\bar{d}_h!)^{-1}$.

Proof: See Appendix E. ∎

Next, we investigate the R-NC. In this scheme, the optimal relay precoder is written by $\hat{\mathbf{B}} = \overline{\mathbf{V}}_g \mathbf{\Delta}_g^{1/2}$ where $\delta_{g,k}$ has the same value with (8). R-NC shows the best performance when no CSI is allowed at the source node. In the following theorem, we quantify the average performance of R-NC.

Theorem 5: The total average BER of R-NC is obtained as

$$\overline{BER}^R_{\text{nc}} = \begin{cases} \left(\bar{\mathcal{C}}_h \cdot P_0\right)^{-\bar{\mathcal{D}}} + o(P_0^{-\bar{\mathcal{D}}}) & \text{if } N_t < N_d; \\ \left(\bar{\mathcal{C}}_{\text{nc}} \cdot P_0\right)^{-\bar{\mathcal{D}}} + o(P_0^{-\bar{\mathcal{D}}}) & \text{if } N_t = N_d, \end{cases}$$

where we denote $\bar{\mathcal{C}}_{\text{nc}} = (\bar{\mathcal{C}}_h^{-\bar{\mathcal{D}}} + \mathcal{C}_{g,\text{nc}}^{-\bar{\mathcal{D}}})^{-1/\bar{\mathcal{D}}}$.

Proof: See Appendix F. ∎

It is remarkable to note that for the case of $N_t < N_d$, both schemes exhibit the identical performance.

A. Discussion

Now we learn from the analysis that the diversity order of R- schemes is given by $\bar{\mathcal{D}} = N_r - N_t + 1$ which is independent of N_d. This result implies that if we design a relaying system

TABLE I
KEY PERFORMANCE PARAMETERS WITH $N_t = N_d = N$

		SR schemes			R- schemes	
		SR-MV	SR-NC	SR-BNC	R-MV	R-NC
Diversity order		$\mathcal{D} = (N_r - N_s + 1)(N - N_s + 1)$			$\mathcal{D} = N_r - N + 1$	
Optimum Relay Location		$\hat{\theta} = 1$			$\hat{\theta} = A^{\frac{1}{1-\zeta\mathcal{D}}}$	$\hat{\theta} = (A/N_t^{\mathcal{D}})^{\frac{1}{1-\zeta\mathcal{D}}}$
G_{adv} (dB)	$N_d \uparrow$	$\frac{10}{\mathcal{D}}\log(1+\theta^{\zeta\mathcal{D}})$			$\frac{10}{\mathcal{D}}\log\left(1+\theta^{\zeta\mathcal{D}}A\right)$	$\frac{10}{\mathcal{D}}\log\left(1+\theta^{\zeta\mathcal{D}}A/N_t^{\mathcal{D}}\right)$
	$N_t \uparrow$	$\frac{10}{\mathcal{D}}\log(1+\theta^{-\zeta\mathcal{D}})$			None	None

with $N_r > N_d$, a higher diversity can be achieved over the MMSE-based $N_t \times N_d$ open-loop MIMO link[4].

Like SR schemes, in case of $N_t = N_d$, the coding gains $\bar{\mathcal{C}}$ and $\bar{\mathcal{C}}_{\text{nc}}$ can be characterized as a quasi-concave function of θ, and thus the global optimal point which maximizes the coding gain is easily obtained as $\hat{\theta} = A^{\frac{1}{1-\zeta\mathcal{D}}}$ and $\hat{\theta} = (A/N_t^{\mathcal{D}})^{\frac{1}{1-\zeta\mathcal{D}}}$ for R-MV and R-NC, respectively. Here A is defined by $A \triangleq a_{g,N_t}/(N_t\bar{a}_h)$ and after some tedious calculations, can be generally expressed as $A = \bar{\mathcal{D}}^{-1} \cdot \binom{N_r}{N_t}$ where $\binom{n}{r} \triangleq \frac{n!}{r!(n-r)!}$. Surprisingly, in R-NC with $\bar{\mathcal{D}} = 1$, i.e., $N_t = N_r$, we get $\hat{\theta} = N_t^{\frac{1}{\zeta-1}} > 1$, since $A = 1$. In other words, the coding gain of R-NC is maximized when the relay node stands closer to the source than the destination.

From Theorem 4 and 5, it is also shown that an increment of N_d creates a non-trivial coding gain advantage over the case of $N_t = N_d$ according to θ. For instance, we can compute the gain of R-MV as $10\log\left(\bar{\mathcal{C}}_h/\bar{\mathcal{C}}\right) = \frac{10}{\mathcal{D}}\log\left(1+\theta^{\zeta\mathcal{D}}A\right)$ dB, which means a substantial performance improvement when the relay is much closer to the source, i.e., $\theta > \hat{\theta}$. Unlike SR schemes, however, the gain would be small at $\theta < \hat{\theta}$, since N_t cannot be greater than N_d.

Also, we see from the analysis that R-NC makes a higher coding gain than R-MV. Setting $\bar{\mathcal{D}} = 1$ and $N_t = N_d$, the performance gap is simply computed by a $10\log\left(\bar{\mathcal{C}}_{\text{nc}}/\bar{\mathcal{C}}\right) = 10\log\left(\frac{1+\theta^{\zeta}}{N_t^{-1}+\theta^{\zeta}}\right)$ dB. As remarked previously, however, R-NC does not offer any performance advantage over R-MV when $N_t < N_d$. Therefore, in this case, it can be said that R-MV is more efficient than R-NC considering the precoding complexity.

For the purpose of the comparison of all schemes presented in this paper, the optimum θ for $N_t = N_d$ and the coding gain advantage (G_{adv}) over $N_t = N_d$ occurred by putting an additional antenna at the source ($N_t \uparrow$) or at the destination ($N_d \uparrow$) are described in Table I. In addition, in Figure 2, we plot the coding gains of R-NC ($\bar{\mathcal{C}}_{\text{nc}}$) and SR-NC ($\mathcal{C}_{\text{nc}}$) in dB scale as a functions of θ. As expected, all curves from R-NC with $N_t = N_d$ exhibit the maximum point at $\theta > 1$ while the optimum θ for SR-NC equals 1. Interestingly, for the case of $N_t = N_d$, R-NC gives the identical performance with SR-NC as the relay gets close to the source, i.e., $\theta > 1$. This is because both $\bar{\mathcal{C}}_{\text{nc}}$ and $\mathcal{C}_{\text{nc}}$ converge to the same value of $\mathcal{C}_{\text{g,nc}}$ as θ increases. In this case, R-NC could be more suitable than SR-NC which requires a larger feedback overhead than R-NC. Our previous discussion about the coding gain advantage over $N_t = N_d$ is also illustrated in this figure. Note that although not presented here, in case of SR-NC, the same result can be drawn for $\theta < 1$ with an additional source antenna. All claims presented in this section will also be confirmed by computer simulations in the following section.

[4]The diversity order of this conventional MIMO system has been derived as $N_d - N_t + 1$ [31] [32]

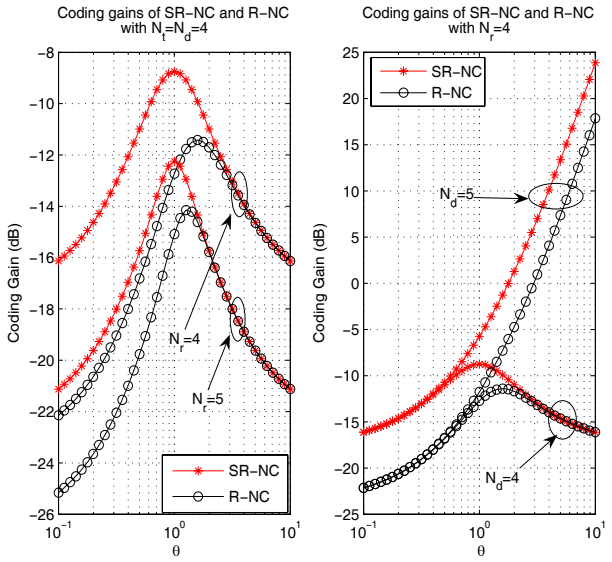

Fig. 2. Coding gain comparison between SR-NC and R-NC as a function of θ in 16 QAM with $N_t = N_s = 4$ and $\zeta = 4$.

V. NUMERICAL RESULTS

In this section, the simulation results are presented to demonstrate the accuracy of the analysis presented in this paper. The numerical results for SR-NC and SR-BNC are plotted employing the algorithm proposed in [8]. We have also adopted the results in [11] for SR-MV and R-MV, and [6] for R-NC. For all simulations, we assumed a flat fading suburban propagation ($\zeta = 4$) channel model.

From Figure 3 to 5, we provide the numerical results for the average BER performance of SR schemes with various system configurations. Since our analysis is fundamentally based on the high SNR assumption, i.e., $P_0 \to \infty$, the accuracy may not be ensured at the low SNR range. Nevertheless, it is clear from these figures that the derived diversity and coding gain expressions precisely reflect the high SNR performance of the average BER curves. Figure 3 describes the BER comparison between all SR schemes with $N_t = N_r = N_d = N_s = 4$ and $\theta = 1$. As illustrated in Section III-D, we confirm that SR-NC and SR-BNC actually achieve the 6 dB and 14.5 dB coding gain advantage over SR-MV.

In Figure 4, we present numerical simulations for SR-MV with $N_t = N_s = 4$ and $\theta = 1$. As expected from Theorem 1, it is clear that for the curves of $N_r = 4$ ($\mathcal{D} = 1$) and $N_r = 5$ ($\mathcal{D} = 2$), the increment of N_d introduces no diversity gain

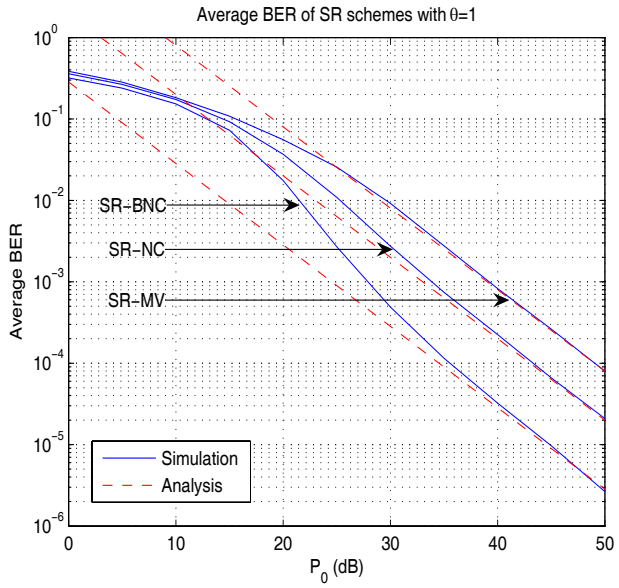

Fig. 3. BER comparison as a function of the total transmit power P_0 in 4 QAM with $N_t = N_r = N_d = N_s = 4$.

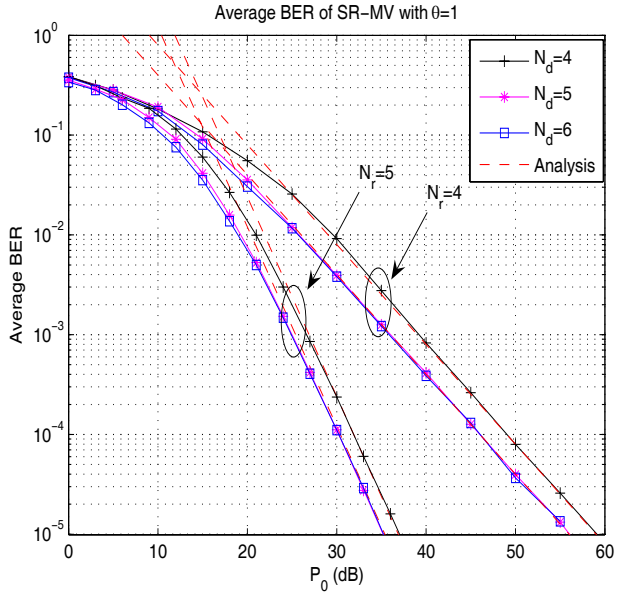

Fig. 4. BER comparison as a function of the total transmit power P_0 in 4 QAM with $N_t = N_s = 4$.

but a $3/\mathcal{D} = 3$ dB and 1.5 dB coding gain advantage over the case of $N_t = N_d$, respectively, regardless of the increased number of antennas.

Figure 5 illustrates the numerical performance of SR-MV considering the effect of relay location. For $N_t = N_r = N_s = 2$ and $N_d \geq 2$, all curves yield the diversity order of 1. As predicted in Section III-D, we observe that for $N_t = N_d$, the coding gain is maximized at $\theta = 1$ and gradually decreases as the relay moves away from the middle point. This figure also illustrates that in this case we can make a much larger coding gain improvement by increasing either N_t or N_d. For instance, we see from the curves with $\theta = 2$ and 5 that the use of $N_d > N_t$ allows a $10\log(1+\theta^4) = 12.3$ dB and 28

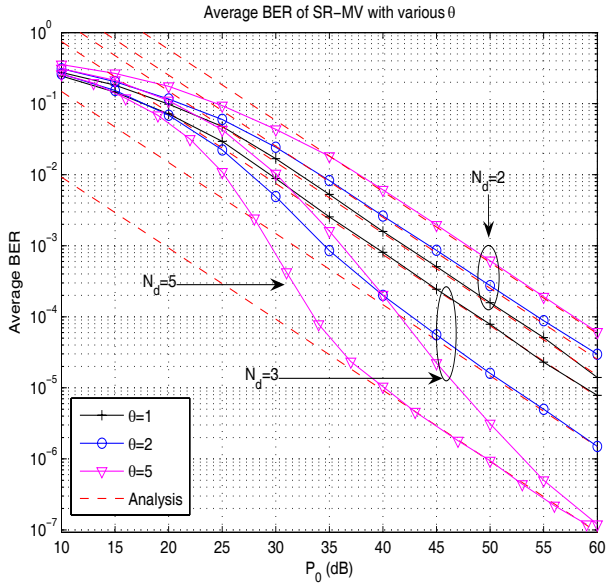

Fig. 5. BER comparison as a function of the total transmit power P_0 in 16 QAM with $N_t = N_r = N_s = 2$.

dB gain, respectively. Note that although not presented in this figure, the same result can be drawn for $\theta = 1/2$ and $1/5$ by increasing N_t from the case of $N_t = N_d$.

One interesting thing we observe in this plot is that as N_d becomes larger, the BER curves with $\theta = 5$ much faster converge to their analytical performance. This can be explained as follows. Let us consider an asymptotic case of $\theta \to \infty$, which leads to $\mathcal{C}_h \to \infty$ and $\mathcal{C}_g \to 0^+$ in Theorem 1. In this case, if $N_t < N_d$, theoretically we can achieve the infinite coding gain $\mathcal{C}_h$. However, as seen from (14) in Appendix B, in order to realize that, we need the infinitely large power P_0 so that the higher order term corresponding to the second hop channel can be ignored. In other words, if P_0 is finite, conversely the second hop would dominate the performance. Consequently, this observation leads to the fact that a large coding gain at $\theta \gg 1$ gives rise to a higher slope $\mathcal{D}_g$ in the medium SNR range.

In Figures 6 and 7, we present the BER performance of R- schemes with $N_t = N_s$. From these figures, we confirm that our analytical results also accurately predict the high SNR performance of R- schemes. Figure 6 depicts the performance of R-MV with different θ. From all curves with $N_d = 2$ and 3, we see that N_d has no impact on the diversity order, but seriously affects the coding gain especially at $\theta > 1$. For example, the curves with $\theta = 2$ actually achieves the gain of $10\log\left(1+\theta^{\zeta}\right) = 12$ dB by an additional antenna at the destination.

Finally, Figure 7 illustrates the performance comparison between R-MV and R-NC with $N_r = N_d = 4$ and $\theta = 1$. Although both R-NC and R-MV yield the same diversity order, we see that R-NC achieves a $10\log\left(\frac{1+\theta^{\zeta}}{N_t^{-1}+\theta^{\zeta}}\right) = 2$ dB gain over R-MV. Also, we verify our previous discussion that when $N_t < N_d$, R-MV may be more efficient than R-NC in terms of the precoding complexity, because both cases exhibit the identical performance.

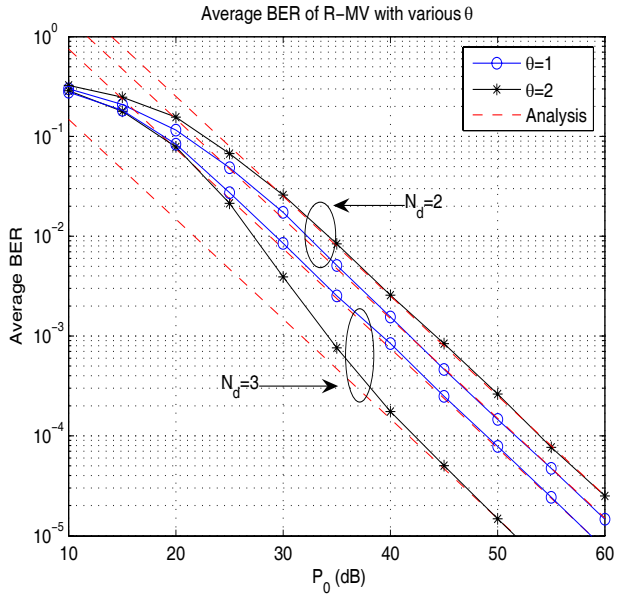

Fig. 6. BER comparison as a function of the total transmit power P_0 in 16 QAM with $N_t = N_r = 2$.

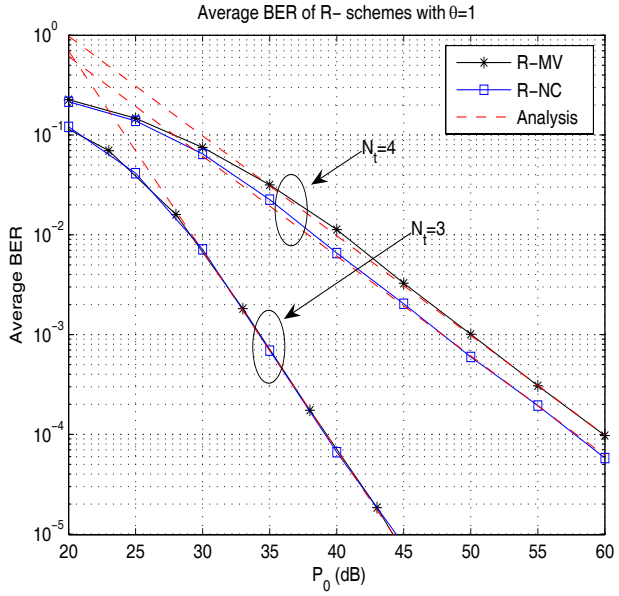

Fig. 7. BER comparison as a function of the total transmit power P_0 in 64 QAM with $N_r = N_d = 4$.

VI. Conclusion

In this paper, we investigated the analytical performance of the average BER in MMSE-based spatial multiplexing MIMO relaying systems. As it is difficult to derive the exact distribution of the channel gain which is given by a harmonic mean of two eigenvalues, we have found an approximated PDF under the high SNR assumption. Then, we have characterized the average BER performance of both the relay only precoding schemes and the source and the relay joint precoding schemes in terms of the coding gain as well as the diversity gain. From the analysis, several interesting observations have been discussed, regarding the relay location and the precoding strategies. Finally, through numerical simulations, we have confirmed that our analytical works accurately predict the numerical performance.

Appendix

A. Proof of Lemma 1

Let $\mathbf{v} = (\lambda_{h,k}, \lambda_{g,k}) \in \mathbb{R}_+^2$. Then we define ρ_{μ_k} as an event that the positive random variable μ_k is near zero, i.e., $\rho_{\mu_k} = \{\mathbf{v} | \mu_k \leq 0^+, \mu_k \in \mathbb{R}_+\}$. Since μ_k is a harmonic mean of $\lambda_{h,k}$ and $\lambda_{g,k}$ as in (4), ρ_{μ_k} can be alternatively expressed as $\rho_{\mu_k} = \rho_{\lambda_{h,k}} \cup \rho_{\lambda_{g,k}}$. Note that there is no other case where μ_k approaches zero. Now, we can assign the probability as $\Pr(\rho_{\mu_k}) = \Pr(\mu_k \leq 0^+) = \Pr(\lambda_{h,k} \leq 0^+) + \Pr(\lambda_{g,k} \leq 0^+) - \Pr(\lambda_{h,k} \leq 0^+, \lambda_{g,k} \leq 0^+)$. Based on these probabilities, the near zero behavior of the cumulative distribution function (CDF) $F_{\mu_k}(\mu_k)$ of μ_k can be obtained as $F_{\mu_k}(\mu_k) = F_{\lambda_{h,k}}(\mu_k) + F_{\lambda_{g,k}}(\mu_k) - F_{\lambda_{h,k}}(\mu_k) F_{\lambda_{g,k}}(\mu_k)$. Then, by taking the derivative, we have the PDF of μ_k as

$$f_{\mu_k}(\mu_k) = f_{\lambda_{h,k}}(\mu_k) + f_{\lambda_{g,k}}(\mu_k) - J(\mu_k), \tag{9}$$

where $J(\mu_k) \triangleq f_{\lambda_{h,k}}(\mu_k) F_{\lambda_{g,k}}(\mu_k) + f_{\lambda_{g,k}}(\mu_k) F_{\lambda_{h,k}}(\mu_k)$. Applying the distributions in (6), the first and second terms of the right-hand side of the equation (9) is computed as $a_{h,k}\mu_k^{d_{h,k}} + a_{g,k}\mu_k^{d_{g,k}} + o(\mu_k^{\min(d_{h,k}, d_{g,k})})$.

Also, applying (6), the term of $J(\mu_k)$ can be rephrased as in (10) at the top of the next page. Here $F_{\lambda_{h,k}}(\mu_k)$ and $F_{\lambda_{g,k}}(\mu_k)$ are monotonically increasing functions of μ_k from the origin, and $d_{h,k} - \min(d_{h,k}, d_{g,k}) \geq 0$ and $d_{g,k} - \min(d_{h,k}, d_{g,k}) \geq 0$. From these facts, it is clear that the equation inside the brace in (10) goes to zero as $\mu_k \to 0^+$, which shows the term $J(\mu_k)$ is $o(\mu_k^{\min(d_{h,k}, d_{g,k})})$, and the proof is completed.

B. Proof of Theorem 1

With the help of studies in [21] and [22], we know that in the conventional one hop link, when the instantaneous SNR γ is given by $\gamma = \bar{\gamma}\mu + \phi$ and the PDF of the channel-dependent parameter μ is first-order expanded as $f_\mu(\mu) = a\mu^d + o(\mu^d)$ where ϕ and $\bar{\gamma}$ designate constants, the average BER in the high SNR region can be parameterized as

$$\begin{aligned} \overline{BER} &= \frac{\alpha}{\log_2 M} \int_0^\infty Q\left(\sqrt{\beta\gamma}\right) f_\mu(\mu) d\mu \\ &= (G_c(\phi, a, d) \cdot \bar{\gamma})^{-(d+1)} + o\left(\bar{\gamma}^{-(d+1)}\right), \end{aligned} \tag{11}$$

where $G_c(\phi, a, d)$ corresponds to a coding gain defined in (7), and $d+1$ is a diversity gain.

Using the above property, we first calculate the average BER of the k-th substream of SR-MV. Plugging the PDF derived in Lemma 1 into the equation (5), we have

$$\overline{BER}_{\text{mv},k} = \frac{\alpha}{\log_2 M} \int_0^\infty Q\left(\sqrt{\beta\gamma_k}\right) f_{\gamma_k}(\gamma_k) d\gamma_k \tag{12}$$

$$\begin{aligned} &= \frac{\alpha}{\log_2 M} \int_0^\infty Q\left(\sqrt{\frac{\beta P_0}{2N_s}\mu_k}\right) f_{\mu_k}(\mu_k) d\mu_k \\ &= \frac{\alpha}{\log_2 M} \left\{ \int_0^\infty Q\left(\sqrt{\frac{\beta P_0}{2N_s}\mu_k}\right) f_{\lambda_{h,k}}(\mu_k) d\mu_k \right. \\ &\qquad \left. + \int_0^\infty Q\left(\sqrt{\frac{\beta P_0}{2N_s}\mu_k}\right) f_{\lambda_{g,k}}(\mu_k) d\mu_k \right\}. \end{aligned} \tag{13}$$

$$J(\mu_k)=\mu_k^{\min(d_{h,k},d_{g,k})}\Bigg\{\Big(a'_{h,k}\mu_k^{d_{h,k}-\min(d_{h,k},d_{g,k})}+o(\mu_k^{d_{h,k}-\min(d_{h,k},d_{g,k})})\Big)F_{\lambda_{g,k}}(\mu_k)$$
$$+\Big(a'_{g,k}\mu_k^{d_{g,k}-\min(d_{h,k},d_{g,k})}+o(\mu_k^{d_{g,k}-\min(d_{h,k},d_{g,k})})\Big)F_{\lambda_{h,k}}(\mu_k)\Bigg\}. \quad (10)$$

Since each term in the above equation represents the BER form of the conventional one hop MIMO link, the average BER of the k-th substream can be easily quantified as

$$\overline{BER}_{\text{mv},k}=\big(\mathcal{C}_{h,k}\cdot P_0\big)^{-(d_{h,k}+1)}+\big(\mathcal{C}_{g,k}\cdot P_0\big)^{-(d_{g,k}+1)}+o\big(P_0^{-(\min(d_{h,k},d_{g,k})+1)}\big), \quad (14)$$

where the coding gain parameters $\mathcal{C}_{h,k}$ and $\mathcal{C}_{g,k}$ are obtained as $\mathcal{C}_{h,k}=\frac{1}{2N_s}G_c(0,a'_{h,k},d_{h,k})$ and $\mathcal{C}_{g,k}=\frac{1}{2N_s}G_c(0,a'_{g,k},d_{g,k})$. From this result, we now see that the total average BER is primarily dominated by the average BER associated with the N_s-th substream, since we have $d_{h,1}>d_{h,2}>\cdots>d_{h,N_s}$ and $d_{g,1}>d_{g,2}>\cdots>d_{g,N_s}$. Accordingly, the performance of SR-MV can be calculated as $\overline{BER}_{\text{mv}}=\frac{1}{N_s}\sum_{k=1}^{N_s}\overline{BER}_{\text{mv},k}\approx\frac{1}{N_s}\overline{BER}_{\text{mv},N_s}$. Similarly, further in the N_s-th substream, $\overline{BER}_{\text{mv},N_s}$ is determined by the term having a smaller order between two terms $\big(\mathcal{C}_{h,N_s}\cdot P_0\big)^{-(d_{h,N_s}+1)}$ and $\big(\mathcal{C}_{g,N_s}\cdot P_0\big)^{-(d_{g,N_s}+1)}$, and finally we prove the theorem.

C. Proof of Lemma 2

As shown in Section III-A, the average error performance of the k-th substream at high SNR is dominated by the channel gain μ_k near the origin. However, if we take all substreams into account, we do not need to consider the case where μ_k goes to zero for $k<N_s$, since its occurrence probability is extremely low compared to the case of $\mu_{N_s}\to 0^+$ as shown in Lemma 1. Therefore, without loss of generality, we can assume that $\mu_k\gg\mu_{N_s}$ for $k<N_s$ when μ_{N_s} is deeply faded.

Now, let us assume $\delta_{h,N_s}>0$ and $\delta_{g,N_s}>0$. Then we observe that in the high SNR regime, the power allocation strategy in (8) is applied such that $\lambda_{h,k}^{1/2}\delta_{h,k}$ and $\lambda_{g,k}^{1/2}\delta_{g,k}$ have the same value for all k. Also, in this case, we can assume that $\lambda_{h,k}\gg\lambda_{h,N_s}$ and $\lambda_{g,k}\gg\lambda_{g,N_s}$ for $k<N_s$, since the average BER primarily depends on the case where λ_{h,N_s} and λ_{g,N_s} experience a deep fading. This result implies that nearly all power resource is allocated on the N_s-th substream as $\delta_{h,N_s}\approx N_s$ and $\delta_{g,N_s}\approx N_s$, which leads to $\gamma_{h,N_s}\approx\frac{P_0}{2}\lambda_{h,N_s}$ and $\gamma_{g,N_s}\approx\frac{P_0}{2}\lambda_{g,N_s}$, respectively. Then it follows $\gamma_{N_s}\approx\frac{P_0}{2}\mu_{N_s}$ and plugging this into (12), we obtain $\overline{BER}_{lb}=(N_s\mathcal{C}_{h,N_s}\cdot P_0)^{-\mathcal{D}_h}+(N_s\mathcal{C}_{g,N_s}\cdot P_0)^{-\mathcal{D}_g}+o(P_0^{-\min(\mathcal{D}_h,\mathcal{D}_g)})$.

Accordingly, the average BER of the N_s-th substream of SR-NC can be expressed and lowerbounded as

$$\begin{aligned}&\overline{BER}_{\text{nc},N_s}\\&=\overline{BER}_{lb}\cdot\Pr(\delta_{h,N_s}>0,\delta_{g,N_s}>0)\\&\quad+\frac{\alpha_{N_s}}{2\log_2 M_{N_s}}(1-\Pr(\delta_{h,N_s}>0,\delta_{g,N_s}>0)) \quad (15)\\&\geq\overline{BER}_{lb},\end{aligned}$$

where the equality holds when $\Pr(\delta_{h,N_s}>0,\delta_{g,N_s}>0)=1$. Also, we can show the following inequality at high SNR as

$$\begin{aligned}&1-\Pr(\delta_{h,N_s}>0,\delta_{g,N_s}>0)\\&=\Pr(\delta_{h,N_s}=0)+\Pr(\delta_{g,N_s}=0)\\&\qquad-\Pr(\delta_{h,N_s}=0)\Pr(\delta_{g,N_s}=0)\\&\leq\Pr\big(\lambda_{h,N_s}\lambda_{h,N_s-1}\leq 4(N_s-1)^2P_0^{-2}\big)\\&\qquad+\Pr\big(\lambda_{g,N_s}\lambda_{g,N_s-1}\leq 4(N_s-1)^2P_0^{-2}\big)\\&\overset{(a)}{\leq}c_1P_0^{-2\mathcal{D}_h}+c_2P_0^{-2\mathcal{D}_g}+o(P_0^{-\min(2\mathcal{D}_h,2\mathcal{D}_g)}),\end{aligned}$$

where c_1 and c_2 designate fixed constants. The proof of the inequality (a) simply follows the approach in [22, Appendix V], which we omit here for the brevity. Substituting this result back in the expression in (15) and canceling higher order terms, we obtain the average BER upper-bound as $\overline{BER}_{\text{nc},N_s}\leq\overline{BER}_{lb}$. This result finally yields $\overline{BER}_{\text{nc},N_s}=\overline{BER}_{lb}$, and the proof is completed.

D. Proof of Theorem 3

First, the average BER of the k-th substream of SR-BNC can be written as $\alpha_k\mathcal{E}[Q(\sqrt{\beta\gamma_k})]/\log_2 M_k$ where the instantaneous SNR γ_k is given by

$$\begin{aligned}\gamma_k&=\sigma_x^2\bigg(\frac{1}{N_s}\sum_{k=1}^{N_s}E_k\bigg)^{-1}-1\\&=\bigg(\frac{1}{N_s}\sum_{k=1}^{N_s}\Big(\frac{1}{\sigma_x^2\lambda_{h,k}\delta_{h,k}+1}+\frac{1}{\sigma_x^2\lambda_{g,k}\delta_{g,k}+1}\Big)\bigg)^{-1}-1.\end{aligned}$$

Here, we have forced all substreams to experience the same MSE. Also we can see that in the high SNR regime, the average BER depends only on the case where λ_{h,N_s} and λ_{g,N_s} are under the deep fading, since the Q-function inside the expectation converges to zero otherwise. In this case, we have $\delta_{h,N_s}\approx N_s$ and $\delta_{g,N_s}\approx N_s$ as shown in Lemma 2, and then it follows

$$\begin{aligned}\gamma_k&=N_s\bigg(\frac{1}{\sigma_x^2N_s\lambda_{h,N_s}+1}+\frac{1}{\sigma_x^2N_s\lambda_{g,N_s}+1}\bigg)^{-1}-1\\&=\frac{N_s^2\sigma_x^4\lambda_{h,N_s}\lambda_{g,N_s}+\sigma_x^2(N_s-1)(\lambda_{h,N_s}+\lambda_{g,N_s})-1}{\sigma_x^2\lambda_{h,N_s}+\sigma_x^2\lambda_{g,N_s}+2}\\&\approx\frac{N_sP_0}{2}\mu_{N_s}+(N_s-1).\end{aligned}$$

Plugging γ_k into the equation (12) and using the result in (11), now the average BER of the k-th substream can be expressed as $\overline{BER}_{\text{bnc},k}=(\mathcal{C}_{h,\text{bnc}}\cdot P_0)^{-\mathcal{D}_h}+(\mathcal{C}_{g,\text{bnc}}\cdot P_0)^{-\mathcal{D}_g}+o(P_0^{-\min(\mathcal{D}_h\mathcal{D}_g)})$ where $\mathcal{C}_{h,\text{bnc}}=\frac{N_s}{2}G_c(\beta(N_s-1),a'_{h,N_s},d_{h,N_s})$ and $\mathcal{C}_{g,\text{bnc}}=\frac{N_s}{2}G_c(\beta(N_s-1),a'_{g,N_s},d_{g,N_s})$. We see that $\overline{BER}_{\text{bnc},k}$ is independent of k, and thus the total average BER of SR-BNC is given by $\overline{BER}_{\text{bnc}}=\overline{BER}_{\text{bnc},k}$.

E. Proof of Theorem 4

For R-MV, the SNR parameters $\gamma_{h,k}$ and $\gamma_{g,k}$ are given by $\gamma_{h,k} = \frac{\sigma_x^2}{(\mathbf{H}^\dagger\mathbf{H}+\sigma_x^{-2}\mathbf{I}_{N_t})^{-1}_{k,k}} - 1 \approx \sigma_x^2\nu_k$, and $\gamma_{g,k} = \sigma_x^2\lambda_{g,k}$, where ν_k is defined as $\nu_k \triangleq 1/\left(\mathbf{H}\mathbf{H}^\dagger\right)^{-1}_{k,k}$. Then we obtain the instantaneous SNR of the k-th substream as $\gamma_k = \sigma_x^2\bar{\mu}_k$, where the channel dependent parameter $\bar{\mu}_k$ is given by $\nu_k\lambda_{g,k}/(\nu_k + \lambda_{g,k})$. The PDF of ν_k can be written as [32] $f_{\nu_k}(\nu_k) = \frac{\eta_h^{-\bar{1}}\exp(-\nu_k/\eta_h)}{\Gamma(N_r-N_t+1)}(\nu_k/\eta_h)^{N_r-N_t}$ for all k where $\Gamma(\cdot)$ denotes the Gamma function defined as $\Gamma(x) = \int_0^\infty t^{x-1}e^{-t}dt$, and first-order expanded as $f_{\nu_k}(\nu_k) = \bar{a}'_h\nu_k^{\bar{d}_h} + o\left(\nu_k^{\bar{d}_h}\right)$, where $\bar{a}'_h = \eta^{-(\bar{d}_h+1)}/\Gamma(\bar{d}_h+1)$ and $\bar{d}_h = N_r - N_t$. Accordingly, following Lemma 1, the PDF of the channel parameter $\bar{\mu}_k$ near the origin can be computed as $f_{\bar{\mu}k}(\bar{\mu}_k) = \bar{a}'_h\bar{\mu}_k^{\bar{d}_h} + a'_{g,k}\bar{\mu}_k^{d_{g,k}} + o\big(\bar{\mu}_k^{\min(\bar{d}_h,d_{g,k})}\big)$, and the average BER of the k-th substream of R-MV is obtained as

$$\overline{BER}^R_{\mathrm{mv},k} = \big(\bar{\mathcal{C}}_h \cdot P_0\big)^{-(\bar{d}_h+1)} + \big(\mathcal{C}_{g,k}\cdot P_0\big)^{-\mathcal{D}_{g,k}} + o\big(P_0^{-\min(\bar{d}_h+1,\mathcal{D}_{g,k})}\big),$$

where $\bar{\mathcal{C}}_h = \frac{1}{2N_t}G_c(0,\bar{a}'_h,\bar{d}_h)$ and $\mathcal{C}_{g,k}$ is defined in Appendix B. Note that the second term does not need to be considered except for $k = N_t$, since $\mathcal{D}_{g,k} > \bar{d}_h + 1$. Thus we arrive at $\overline{BER}^R_{\mathrm{mv},k} = \big(\bar{\mathcal{C}}_h \cdot P_0\big)^{-(\bar{d}_h+1)} + o\big(P_0^{-(\bar{d}_h+1)}\big)$ for $k < N_t$. Using this result, finally we can calculate the total average BER of R-MV as $\overline{BER}^R_{\mathrm{mv}} = \frac{1}{N_s}\sum_{k=1}^{N_s}\overline{BER}^R_{\mathrm{mv},k}$.

F. Proof of Theorem 5

The SNR parameter $\gamma_{h,k}$ is equal to $\sigma_x^2\nu_k$ defined in Appendix E, and from the result in Lemma 2, $\gamma_{g,k}$ can be written as $\frac{P_0}{2}\lambda_{g,k}$. Then we have the instantaneous SNR of the k-th substream as $\gamma_k = \frac{P_0}{2N_t}\hat{\mu}_k$ where $\hat{\mu}_k = \nu_k N_t\lambda_{g,k}/(\nu_k + N_t\lambda_{g,k})$. By Lemma 1, the PDF of $\hat{\mu}_k$ is obtained as $f_{\hat{\mu}_k}(\hat{\mu}_k) = \bar{a}'_h\hat{\mu}_k^{\bar{d}_h} + N_t^{-(d_{g,k}+1)}a'_{g,k}\hat{\mu}_k^{d_{g,k}} + o\big(\hat{\mu}_k^{\min(\bar{d}_h,d_{g,k})}\big)$, and the average BER of the k-th substream of R-NC is written by

$$\overline{BER}^R_{\mathrm{nc},k} = \big(\bar{\mathcal{C}}_h \cdot P_0\big)^{-(\bar{d}_h+1)} + \big(N_t\mathcal{C}_{g,k}\cdot P_0\big)^{-\mathcal{D}_{g,k}} + o\big(P_0^{-\min(\bar{\mathcal{D}},\mathcal{D}_{g,k})}\big).$$

As shown in Appendix E, we have $\overline{BER}^R_{\mathrm{nc},k} = (\bar{\mathcal{C}}_h \cdot P_0)^{-(\bar{d}_h+1)} + o(P_0^{-(\bar{d}_h+1)})$ for $k < N_t$. Hence, we finally get the total average BER of R-NC using the metric, $\overline{BER}^R_{\mathrm{nc}} = \frac{1}{N_s}\sum_{k=1}^{N_s}\overline{BER}^R_{\mathrm{nc},k}$.

REFERENCES

[1] I. E. Telatar, "Capacity of multi-antenna Gaussian channels," *Eur. Trans. Telecommun.*, vol. 10, pp. 585–595, Nov. 1999.

[2] H. Lee and I. Lee, "New approach for error compensation in coded V-BLAST OFDM systems," *IEEE Trans. Commun.*, vol. 55, no. 2, pp. 345–355, Feb. 2007.

[3] B. Wang, J. Zhang, and A. Host-Madsen, "On the capacity of MIMO relay channels," *IEEE Trans. Inf. Theory*, vol. 51, pp. 29–43, Jan. 2005.

[4] H. Bolcskei, R. U. Nabar, O. Oyman, and A. J. Paulraj, "Capacity scaling laws in MIMO relay networks," *IEEE Trans. Wireless Commun.*, vol. 5, pp. 1433–1444, June 2006.

[5] J. Laneman, D. Tse, and G. W. Wornell, "Cooperative diversity in wireless networks: efficient protocols and outage behavior," *IEEE Trans. Inf. Theory*, vol. 50, pp. 3062–3080, Dec. 2004.

[6] W. Guan and H. Luo, "Joint MMSE transceiver design in non-regenerative MIMO relay systems," *IEEE Commun. Lett.*, vol. 12, pp. 517–519, July 2008.

[7] C. Li, X. Wang, L. Yang, and W.-P. Zhu, "A joint source and relay power allocation scheme for a class of MIMO relay systems," *IEEE Trans. Signal Process.*, vol. 57, pp. 4852–4860, Dec. 2009.

[8] Y. Rong, X. Tang, and Y. Hua, "A unified framework for optimizing linear non-regenerative multicarrier MIMO relay communication systems," *IEEE Trans. Signal Process.*, vol. 57, pp. 4837–4851, Dec. 2009.

[9] R. Mo and Y. H. Chew, "MMSE-based joint source and relay precoding design for amplify-and-forward MIMO relay networks," *IEEE Trans. Wireless Commun.*, vol. 8, pp. 4668–4676, Sep. 2009.

[10] K.-J. Lee, H. Sung, E. Park, and I. Lee, "Joint optimization for one and two-way MIMO AF multiple-relay systems," *IEEE Trans. Wireless Commun.*, vol. 9, pp. 3671–3681, Dec. 2010.

[11] C. Song, K.-J. Lee, and I. Lee, "MMSE based transceiver designs in closed-loop non-regenerative MIMO relaying systems," *IEEE Trans. Wireless Commun.*, vol. 9, pp. 2310–2319, July 2010.

[12] C. Song and I. Lee, "Diversity analysis of coded beamforming in MIMO-OFDM amplify-and-forward relaying systems," *IEEE Trans. Wireless Commun.*, vol. 10, pp. 2445–2450, Aug. 2011.

[13] M. O. Hasna and M.-S. Alouini, "End-to-end performance of transmission systems with relays over Rayleigh-fading channels," *IEEE Trans. Wireless Commun.*, vol. 2, pp. 1126–1131, Nov. 2003.

[14] M. O. Hasna and M.-S. Alouini, "Harmonic mean and end-to-end performance of transmission systems with relays," *IEEE Trans. Commun.*, vol. 52, pp. 130–135, Jan. 2004.

[15] G. K. Kragiannidis, T. A. Tsiftsis, and R. K. Mallik, "Bounds for multihop relayed communications in Nakagami-m fading," *IEEE Trans. Commun.*, vol. 54, pp. 18–22, Jan. 2006.

[16] T. A. Tsiftsis, G. K. Karagiannidis, P. T. Mathiopoulos, and S. A. Kotsopoulos, "Nonregenerative dual-hop cooperative links with selection diversity," *Eurasip J. Wireless Commun. Netw.*, pp. 1–8, 2006.

[17] H. Min, S. Lee, and K. Kwak, "Effect of multiple antennas at the source on outage probability for amplify-and-forward relaying systems," *IEEE Trans. Wireless Commun.*, vol. 8, pp. 633–637, Feb. 2009.

[18] R. H. Y. Louie, Y. Li, H. A. Suraweera, and B. Vucetic, "Performance analysis of beamforming in two hop amplify and forward relay networks with antenna correlation," *IEEE Trans. Wireless Commun.*, vol. 8, pp. 3132–3141, June 2009.

[19] D. B. da Costa and S. Aissa, "Cooperative dual-hop relaying systems with beamforming over Nakagami-m fading channels," *IEEE Trans. Wireless Commun.*, vol. 8, pp. 3950–3954, Aug. 2009.

[20] B. Khoshnevis, W. Yu, and R. Adve, "Grassmannian beamforming for MIMO amplify-and-forward relaying," *IEEE J. Sel. Areas Commun.*, vol. 26, pp. 1397–1407, Oct. 2008.

[21] Z. Wang and G. B. Giannakis, "A simple and general parameterization quantifying performance in fading channels," *IEEE Trans. Commun.*, vol. 51, pp. 1389–1398, Aug. 2003.

[22] L. G. Ordonez, D. P. Palomar, A. Pages-Zamora, and J. R. Fonollosa, "High-SNR analytical performance of spatial multiplexing MIMO systems with CSI," *IEEE Trans. Signal Process.*, vol. 55, pp. 5447–5463, Nov. 2007.

[23] S. Haykin and M. Moher, *Modern Wireless Communications*. Pearson Prentice Hall, 2005.

[24] Y. Fan and J. Thompson, "MIMO configurations for relay channels: theory and practice," *IEEE Trans. Wireless Commun.*, vol. 12, pp. 1774–1786, May 2007.

[25] D. P. Palomar, J. M. Cioffi, and M. A. Lagunas, "Joint Tx-Rx beamforming design for multicarrier MIMO channels: a unified framework for convex optimization," *IEEE Trans. Signal Process.*, vol. 51, pp. 2381–2401, Sep. 2003.

[26] A. Scaglione, P. Stoica, S. Barbarossa, G. B. Giannakis, and H. Sampath, "Optimal designs for space-time linear precoders and decoders," *IEEE Trans. Signal Process.*, vol. 50, pp. 1051–1064, May 2002.

[27] J. M. Cioffi, "379A Class Note: Signal Processing and Detection, Stanford University, CA.

[28] T. Taniguchi, S. Sha, and Y. Karasawa, "Analysis and approximation of statistical distribution of eigenvalues in i.i.d. MIMO channels under Rayleigh fading," *IEICE Trans. Fundamentals*, vol. E91-A, pp. 2808–2817, Oct. 2008.

[29] E. Sengul, E. Akay, and E. Ayanoglu, "Diversity analysis of single and multiple beamforming," *IEEE Trans. Commun.*, vol. 54, pp. 990–993, June 2006.

[30] S. Boyd and L. Vandenberghe, *Convex Optimization*. Cambridge University Press, 2004.

[31] N. Kim, Y. Lee, and H. Park, "Performance analysis of MIMO system with linear MMSE receiver," *IEEE Trans. Wireless Commun.*, vol. 7, pp. 4424–4478, Nov. 2008.
[32] D. Gore, R. W. Heath, and A. Paulraj, "On the performance of the zero forcing receiver in presence of transmit correlation," in *Proc. IEEE ISIT '02*, p. 159, July 2002.

Changick Song (S'09) received the B.S. and M.S. degrees in electrical engineering from Korea University, Seoul, Korea, in 2007 and 2009, where he is currently working toward the Ph.D. degree in the School of Electrical Engineering. During the winter of 2009, he visited University of Southern California, Los Angeles, CA, USA to conduct a collaborative research. His research interests include information theory and signal processing for wireless communications such as the MIMO-OFDM system and the wireless relay network. He received the 2011 Best Graduate Student Paper Award in Korea University.

Kyoung-Jae Lee (S'06-M'11) received the B.S., M.S., and Ph.D. degrees in the School of Electrical Engineering from Korea University, Seoul, Korea, in 2005, 2007, and 2011, respectively. He worked as an intern at Beceem Communications, Santa Clara, CA, USA during the winter of 2006, and visited University of Southern California, Los Angeles, CA, USA to conduct a collaborative research during the summer of 2009. From March 2011 to September 2011, he was a Postdoctoral fellow in Korea University. Since October 2011, he has been with the Wireless Networking and Communications Group at the University of Texas at Austin, TX, USA, where he is currently a Postdoctoral researcher. His research interests are in communication theory and signal processing for wireless communications, including MIMO-OFDM systems and relay networks. He received the Gold Paper Award at the IEEE Seoul Section Student Paper Contest in 2007, and the Best Paper Award at the IEEE VTC fall in 2009.

Inkyu Lee (S'92-M'95-SM'01) received the B.S. degree (Hon.) in control and instrumentation engineering from Seoul National University, Seoul, Korea, in 1990, and the M.S. and Ph.D. degrees in electrical engineering from Stanford University, Stanford, CA, in 1992 and 1995, respectively. From 1991 to 1995, he was a Research Assistant at the Information Systems Laboratory, Stanford University. From 1995 to 2001, he was a Member of Technical Staff at Bell Laboratories, Lucent Technologies, where he studied the high-speed wireless system design. He later worked for Agere Systems (formerly Microelectronics Group of Lucent Technologies), Murray Hill, NJ, as a Distinguished Member of Technical Staff from 2001 to 2002. In September 2002, he joined the faculty of Korea University, Seoul, Korea, where he is currently a Professor in the School of Electrical Engineering. During 2009, he visited University of Southern California, LA, USA, as a visiting Professor. He has published over 60 journal papers in IEEE, and has 30 U.S. patents granted or pending. His research interests include digital communications, signal processing, and coding techniques. Dr. Lee currently serves as an Associate Editor for IEEE TRANSACTIONS ON COMMUNICATIONS and the IEEE TRANSACTIONS ON WIRELESS COMMUNICATIONS. Also, he has been a Chief Guest Editor for the IEEE JOURNAL ON SELECTED AREAS IN COMMUNICATIONS (Special Issue on 4G Wireless Systems). He received the IT Young Engineer Award as the IEEE/IEEK joint award in 2006. Also he received the Best Paper Award at APCC in 2006 and IEEE VTC in 2009.